Journal of Molecular Catalysis A: Chemical 316 (2010) 100–105

Contents lists available at ScienceDirect

Journal of Molecular Catalysis A: Chemical

journal homepage: www.elsevier.com/locate/molcata

Gold catalysts supported on the mesoporous nanoparticles composited of zirconia and silicate for oxidation of formaldehyde

Yanbing Zhang[a], Yuenian Shen[a], Xuzhuang Yang[a], Shishan Sheng[b], Tana Wang[a], Moses F. Adebajo[c], Huaiyong Zhu[c,*]

[a] College of Chemistry and Chemical Engineering, Inner Mongolia University, Hohhot 010021, PR China
[b] State Key Laboratory of Catalysis, Dalian Institute of Chemical Physics, The Chinese Academy of Sciences, Dalian 116023, PR China
[c] School of Physical and Chemical Sciences, Queensland University of Technology, Brisbane, QLD 4001, Australia

ARTICLE INFO

Article history:
Received 6 February 2009
Received in revised form 20 May 2009
Accepted 5 October 2009
Available online 12 October 2009

Keywords:
Gold catalyst
Mesoporous support
Formaldehyde oxidation
Adsorption
Nanoparticle

ABSTRACT

Gold was loaded onto porous nanocomposite of ZrO_2 and silicate by deposition–precipitation. The resulting Au/ZrO_2-nanocomposites are found to be superior catalysts for removal of formaldehyde from indoor air at moderate temperature by oxidation. They have large specific surface areas and allow the gold to be adequately dispersed as small nanoparticles (NPs). According to the analysis of transmission electron microscopy (TEM) and X-ray photoelectron spectroscopy (XPS), in the as-prepared catalyst, gold was well dispersed and in an oxidized state of Au^{3+}; and it was reduced to metallic crystals (Au^0) during its use as catalyst. The temperature programmed desorption (TPD) results show that gold species in the two states strongly adsorb HCHO molecules at ambient temperature. The adsorbed HCHO molecules convert rapidly into formate species, as observed by the infrared spectra. The temperature programmed surface reaction (TPSR) study reveals that at temperatures below 450 K, the HCHO oxidation involves reaction between adsorbed formate species and adsorbed oxygen molecules. This explains why the gold species in both states are the active sites for HCHO oxidation, and also indicates that HCHO adsorption on the gold species and oxygen adsorption on the support are crucial steps for the oxidation.

1. Introduction

Supported gold catalysts exhibit superior catalytic activity at low temperature for the oxidation of various volatile organic compounds (VOCs) [1–7]. These catalysts have attracted considerable research interests and several reviews have been published [8–11]. The gold catalysts that are active at ambient temperature have potential to be used for cleaning air in particular the indoor air. Gold catalyst is generally loaded onto a metal oxide support for two major reasons: firstly, if the support has a large specific surface area, gold can disperse over the support surface in small species (fine crystal even clusters) [12–14]. The small gold particle size is crucial for a better activity because there are more active sites on the gold catalyst; secondly, there is interaction between gold species and metal oxide support, and this interaction can enhance the catalytic performance of the catalyst [15]. Fine metal oxide powders have large specific surface area, and thus are potential supports for gold catalyst with high activity. However, uses of fine metal oxide powders often involve serious agglomeration of the fine powders and loss of the powders during the reaction. Recently, we developed mesoporous nanocomposite structures of metal oxide and silicate from an inorganic salt of transition metal and layered clay laponite [16,17]. These nanocomposites have large pore size and metal oxides existing in nanocrystal so that the active component, such as gold, can be loaded on the surface of the metal oxide nanocrystals readily by a deposition–precipitation method.

Formaldehyde (HCHO) is a serious pollutant of the indoor air, which is often used in room decorating and refurbishing process, as well as in furniture production [18]. It can be gradually released from furniture, decorating materials and urea-formaldehyde resin products as a harmful gas. HCHO may cause skin disease if it irritates our skin and bronchitis or swallow disease if in haled [19,20], and its carcinogenicity was also reported [21]. To remove low concentration HCHO from indoor air, two methods are ideal from the practical and economic point of view: oxidizing HCHO to carbon dioxide through a catalytic process at moderate temperature in air and adsorbing HCHO by an efficient adsorbent at ambient temperature [22–27]. To remove very low concentration HCHO (at the level of parts per million), the catalytic oxidation is believed to be an effective approach [28]. We have conducted a series studies on catalysts of gold supported on metal oxides for HCHO oxidation

* Corresponding author at: School of Physical and Chemical Sciences, Queensland University of Technology, E-503B, Garden Points Campus, Brisbane, QLD 4001, Australia. Tel.: +61 7 3864 1581; fax: +61 7 3864 1804.
E-mail addresses: ceshen@mail.imu.edu.cn (Y. Shen), sssheng@dicp.ac.cn (S. Sheng), hy.zhu@qut.edu.au (H. Zhu).

1381-1169/$ – see front matter © 2009 Elsevier B.V. All rights reserved.
doi:10.1016/j.molcata.2009.10.006

[29–31], and found that the complete oxidation temperature was achieved near room temperature.

In the present study, ZrO_2-nanocomposite with a mesoporous structure and large specific surface area was used as support, and various amounts of gold were loaded onto the support by a deposition–precipitation approach. The pore diameter and the pore size distribution were determined by the nitrogen adsorption–desorption. XRD, TEM, XPS, etc. were used to study the structure of catalyst. TPD and TPSR were used to study the performance of adsorbing HCHO and the catalysis of oxidizing HCHO. The catalytic activity of HCHO oxidation on those catalysts was investigated.

2. Experimental

2.1. Preparation of support and catalysts

2.1.1. Materials

A synthetic layered clay laponite (Laponite RD), supplied by Fernz Specialty Chemicals, Australia was used as received. The clay powder has a BET specific surface area of 370 m^2/g and a cation exchange capacity of 55 meq per 100 g of clay. $ZrOCl_2$ and a nonionic polyethylene oxide (PEO) surfactant, Tergitol 15S-7, were used as received from Aldrich in this study. The chemical formula of the surfactant is $C_{12-14}H_{25-29}O(CH_2CH_2O)_7H$. Analytical grade $HAuCl_4$ was supplied by Beijing Chemical Reagent Co. Ltd, China

2.1.2. Support preparation

The highly porous ZrO_2-nanocomposite was prepared from $ZrOCl_2$ solution and laponite [16,32]. An aqueous $ZrOCl_2$ solution was refluxed for a few hours. 4.0 g of laponite was dispersed into 200 ml of deionized water to form a suspension. To increase the porosity of the support, 8.0 g of the PEO surfactant was added into the laponite dispersion. To this mixture, the refluxed $ZrOCl_2$ solution was added dropwise with continuous stirring. After stirring for a further 3 h, the suspension was transferred into an autoclave and maintained at 373 K for 2 days. A white precipitate was recovered from the mixture and washed with deionized water until it was free from Cl^- ions according to a test with $AgNO_3$. The wet cake was dried in air and calcined at 773 K for 20 h. The PEO surfactant acts as space filler, and removal of the surfactant during the calcination created large porosity in the final support.

2.1.3. Loading gold

Supported gold catalysts were generally prepared by deposition–precipitation and co-precipitation methods [33]. In the present work, gold was loaded by deposition–precipitation. Different amounts of gold were loaded onto the support by varying the volume of the 2.94 mmol/L $HAuCl_4$ solution used in this procedure. A dilute of NaOH solution (0.05 mol/L) was added into different suspensions slowly to increase the pH to 8, and subsequently the suspension was left for a few hours. The solid in the suspension was then recovered, washed with deionized water until it was free from Cl^- ions, and dried in air at 333 K. The gold loading experiment was carried out at ambient temperature and the obtained solids were dried at low temperature in order to avoid the change of gold species in oxidation state. The gold content in the catalysts was determined by ICP-AES measurement.

2.2. Catalytic activity test

The catalytic activity of the catalysts for oxidation of HCHO was assessed on a glass tubular reactor equipped with a temperature controller. The inner diameter of the reactor was 8 mm and generally 200 mg of catalyst (40–60 mesh) was loaded into it. Purified air was used to carry HCHO to the reactor, which passed through a vessel containing 5 Å molecular sieve and NaOH pellets in order to remove H_2O and CO_2 in air. The air then passed through a HCHO solution container and carried HCHO to the reactor. The container was kept at 273 K using a mixture of water and ice. The gas hourly space velocity (GHSV) was controlled at 52,000 ml h^{-1} g^{-1} (catal.) by a mass flow controller in the experiment. The HCHO concentration entering the glass reactor is constant, about 90 mg per cubic meter of air measured by the spectrophotometric method which, HCHO in air being adsorbed by a phenol agent [$C_6H_4SN(CH_3)C{:}NNH_2{\cdot}HCl$] adsorbing liquid, is a convenient measurement for HCHO in air.

The reaction product, CO_2, was analyzed by a FQ-W type IR analyzer (FQ-W-CO_2, Fushan Analyzer Co. Ltd, China) which can detect the CO_2 concentration as low as 2 ppm. A Shimadzu GC-8A gas chromatograph (GC) was used to determine the reaction products other than CO_2, such as HCOOH and CO, which was equipped with a GDX-403 packed column (at 383 K) and a TCD detector (at 433 K). The lowest detectable concentration of HCHO or HCOOH by the GC-TCD system is 10 ppm.

2.3. Catalyst characterization

Gold content of the catalysts was determined by ICP-AES (Haiguang WLY100-1, Beijing Kechuang Haiguang Instrument Co. Ltd.). The gold contents were 0.06 wt.% (0.06Au), 0.73 wt.% (0.73Au) and 0.85 wt.% (0.85Au) respectively. Among them 0.85 wt.% was the highest content achieved by this work for the Au/ZrO_2-nanocomposite catalysts. The oxidation state of the gold species in the catalysts was characterized by X-ray photoelectron spectroscopy (XPS, VG ESCALAB MK-2) using Al Kα radiation (1486.6 eV). The voltage and power for the measurements were 12.5 kV and 250 W, respectively. The vacuum in the test chamber during the collection of spectra was maintained at 2×10^{-10} mbar. The binding energies were calibrated for the surface charge by referencing to the C_{1S} peak of the contaminant carbon at 284.6 eV. Transmission electron microscopy was used to study the configuration of gold species in the catalyst. TEM was carried out on a JEM 2010 microscope operating at 200 kV.

X-ray diffraction measurements were carried out on a BRUKER AXS-D8 diffractometer using Cu Kα radiation, 40 kV, 20 mA. Nitrogen adsorption–desorption isotherms were obtained on a Micromeritics Instrument Corporation at −196.6 °C over a wide relative pressure range from 0 to 0.98. The samples were degassed under vacuum for several hours before nitrogen adsorption measurements. The pore diameter and the pore size distribution were derived by BJH method. The specific surface area was calculated by BET method and the nitrogen adsorption data of the sample in a P/P_0 range between 0.05 and 0.2.

Temperature programmed desorption of HCHO was carried out in a U shape glass tube. About 0.1 g catalyst (0.73Au) was loaded into the tube and then high purity nitrogen was passed through the catalyst and the temperature of glass tube was risen to 400 K to remove the adsorbed gas on the catalyst. Then the temperature was lowered to ambient temperature and flow of high purity nitrogen carrying HCHO passed through the glass tube for 10 min to allow formaldehyde to be adsorbed on the surface of the catalyst. Afterward the gas passing through the catalyst was switched to high purity nitrogen only, followed by raising the temperature according to a program. The effluent from glass reactor was analyzed by a formaldehyde analyzer INTERSCAN 4160 (made in USA) least digit 0.01 ppm, error-detecting $\leq \pm 0.02$ ppm.

Temperature programmed surface reaction (TPSR) experiments were conducted to acquire the information of the reaction between the adsorbed species, HCHO molecules and oxygen. In these experiments about 0.2 g of the sample (0.73Au) was loaded in the reactor, and purged with high purity nitrogen (99.995%) whilst the tem-

perature of the reactor was increased linearly from ambient to 423 K in order to remove the substances absorbed on the surface of the samples. The samples were then cooled down to the ambient temperature in the flow of high purity nitrogen, followed by introduction of HCHO and H_2O carried by purified air or high purity nitrogen into the reactor. The HCHO flowed though the reactor for 10 min, allowing the substances involved to adsorb on the catalysts. Subsequently, the samples were purged with high purity nitrogen for 30 min to remove unabsorbed molecules in the reactor, and the temperature of the reactor was increased at a designed rate in a flow of high purity nitrogen or purified air to allow the oxidation reaction to take place. The oxidation product, CO_2 in the effluent gas from the reactor was analyzed by an IR CO_2 analyzer on line. There were two possible sources of the oxidant, O_2, during the oxidation: from oxygen absorbed on the surface of the catalyst and from the lattice oxygen of support. If the oxidation is conducted in a nitrogen flow, the oxidant of the reaction is from the support.

3. Results

3.1. The structure of the support

Fig. 1a is the XRD pattern of the support, ZrO_2-nanocomposite. There are no significant diffraction peaks except a broadened peak located in the 2θ range of 20–40°, which is consisted of the diffraction peak 0 1 1 (2θ = 24.1°), $\bar{1}$ 1 0 (2θ = 24.5°), $\bar{1}$ 1 1 (2θ = 28.2°) and 1 1 1 (2θ = 31.5°), 0 0 2 (2θ = 34.2°), 0 2 0 (2θ = 34.5°) and 2 0 0 (2θ = 35.3°) of the monoclinic ZrO_2, indicating the presence of poorly crystallized ZrO_2, which should be very small crystals, in the support. The support is composite structure of ZrO_2 nanoparticles and silicate [34–36]. Fig. 1b is the XRD patterns of the catalyst of gold supported on the ZrO_2-nanocomposite with a gold content of 0.73 wt.%. No diffraction peaks of gold metal can be observed because of the low gold content.

The nitrogen adsorption–desorption isotherms of samples Au/ZrO_2-nanocomposite (0.73 wt.%Au) and ZrO_2-nanocomposite are shown in Fig. 2. The BET specific surface area and the pore volume of the samples are listed in Table 1. Apparently, the specific surface area and pore volume of ZrO_2-nanocomposite are far larger than that of the starting clay, laponite. Loading gold to the support caused slight changes in both the specific surface area and pore volume because the small quantity of the loaded gold does not remarkably influence the pore structure of support. The BJH pore size distributions of the two samples are shown in Fig. 3.

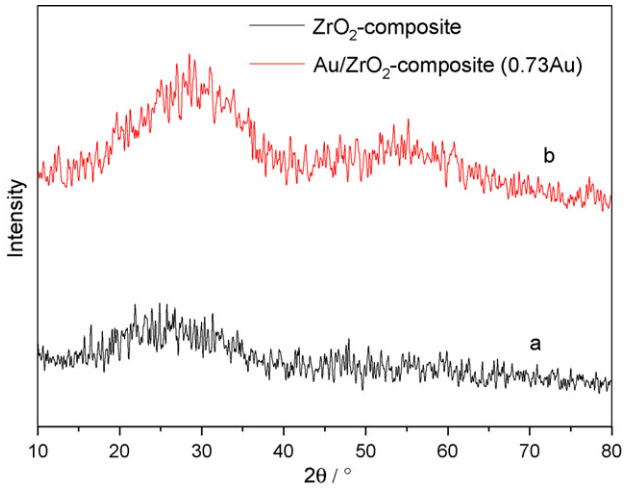

Fig. 1. XRD patterns of ZrO_2-nanocomposite (a) and Au/ZrO_2-nanocomposite containing 0.73 wt.% Au (b).

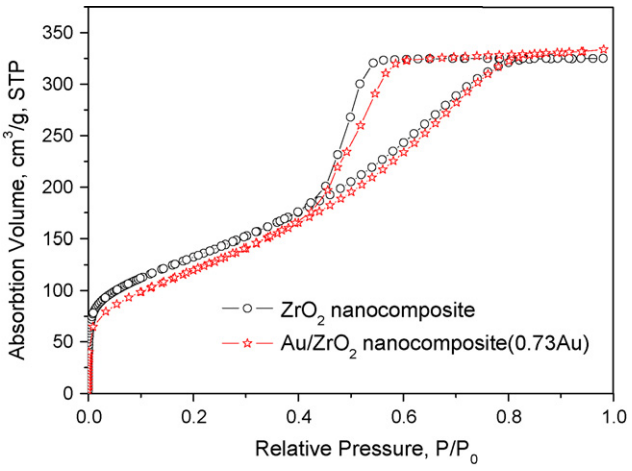

Fig. 2. N_2 adsorption and desorption isotherms of samples ZrO_2-nanocomposite and Au/ZrO_2-nanocomposite containing 0.73 wt.% Au.

Table 1
Specific surface area (BET S.A.) and pore volume (Vp) of the samples.

Sample name	BET S.A. (m^2/g)	Vp (cm^3/g)
Laponite	370	0.263
ZrO_2-nanocomposite	473	0.503
Au/ZrO_2-nanocomposite (0.73Au)	447	0.516

Obviously, there are abundant mesopores in the two samples and the pore size distribution of sample Au/ZrO_2-nanocomposite is broader than that of sample ZrO_2-nanocomposite. From Fig. 2, it can be noticed that at low relative pressures ($P/P_0 < 0.1$), the adsorption of Au/ZrO_2-nanocomposite (0.73 wt.%) is lower than that of ZrO_2-nanocomposite. As the adsorption at low relative pressures is mainly from micropores, the result suggests smaller specific surface area and pore volume from the micropores in sample Au/ZrO_2-nanocomposite (0.73 wt.%). Accordingly, during the gold loading process, some gold species blocks the tunnels, which makes the decrease of the specific surface area of the sample.

3.2. Catalytic activity

The catalytic activities of the Au/ZrO_2-nanocomposite catalysts (with gold content 0.85 wt.%, 0.73 wt.% and 0.06 wt.%) and the ZrO_2-nanocomposite support at different temperatures are illustrated

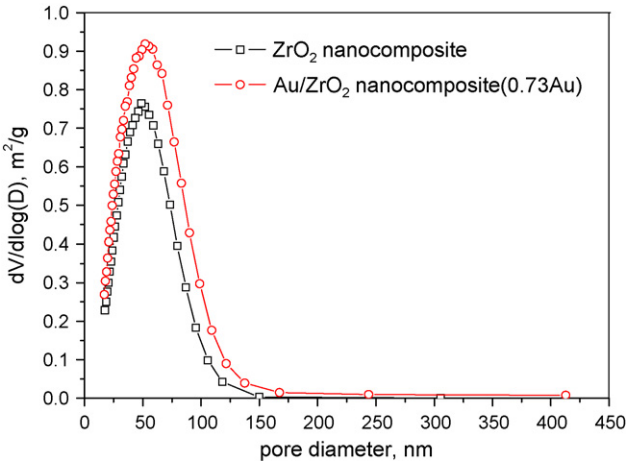

Fig. 3. BJH pore size distribution of samples ZrO_2-nanocomposite and Au/ZrO_2-nanocomposite containing 0.73 wt.% Au.

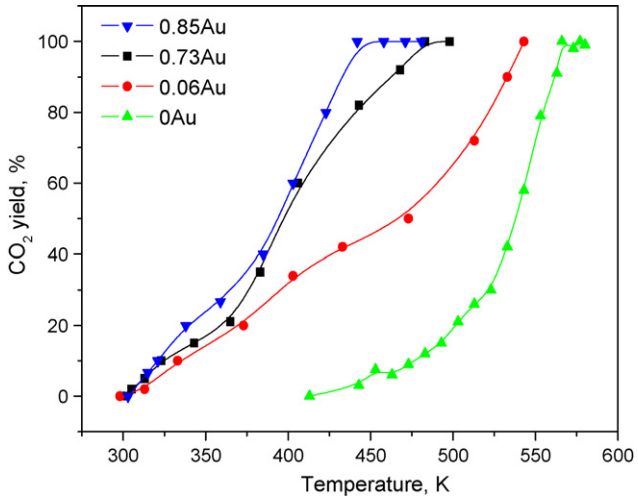

Fig. 4. The catalytic activities of the catalysts with different gold contents. The activity is expressed in the yield of CO_2. The operating conditions are: GHSV = 52,000 ml $h^{-1}g^{-1}$ (catal.), 200 mg catalyst (40–60 mesh).

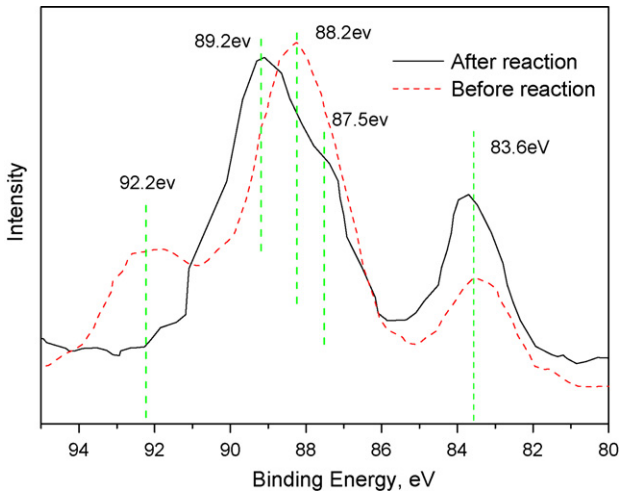

Fig. 5. The XPS in Au 4*f* region for Au/ZrO_2-nanocomposite containing 0.73 wt.% Au before and after reaction.

in Fig. 4 in which the concentration of CO_2 in effluent gas from reactor is used to indicate the activity of HCHO oxidation. This is because CO_2 and H_2O are the only reaction products and no other by-products, such as the HCOOH and CO, can be found in the effluents by GC measurement.

The supported Au/ZrO_2-nanocomposite catalysts exhibit very good activity, compared to the support ZrO_2-nanocomposite alone. Even the catalyst with gold content as low as 0.06 wt.% appears much more active than the support: considerable CO_2 yield can be observed on this catalyst below 400 K, while there is little CO_2 produced over the support at such low temperatures. Generally, at a higher temperature, more HCHO molecules are oxidized to CO_2, resulting in a higher CO_2 yield. This observation is consistent with the results of GC measurement (not shown), HCHO content in the effluent decreasing with the increase of the reaction temperature. For the gold catalysts in this study, the higher the gold content, the lower the temperature at which the complete oxidation (CO_2 yield = 100%) is achieved. At a fixed reaction temperature, the CO_2 yield increases with the rise of gold content in catalysts. The fact that the activity of the catalyst increases with increase of gold content suggests that gold species on the ZrO_2-nanocomposite must play a central role for HCHO oxidation below 450 K. On the supported catalyst with gold content of 0.85 wt.%, the HCHO oxidation has a light-off temperature (10% of conversion) of ~325 K that is close to the ambient temperature. The complete oxidation temperature for this catalyst is at 430 K. In contrast, a much higher light-off temperature of ~450 K is observed for the support without gold, and the complete HCHO oxidation is achieved at 560 K. It is a key issue for removal of the indoor air pollutant HCHO that the oxidation can take place at temperatures close to the ambient temperature. Therefore, the catalysts of gold on mesoporous support of ZrO_2-nanocomposite have potential to be an efficient catalyst for the removal of HCHO pollutant in indoor air.

3.3. Oxidation state of gold in the catalysts

Although there are controversial arguments on the effects of oxidation state of gold species on the reaction in literatures, many researchers believe that the oxidation state of gold in catalysts has an important influence on the catalytic activity [37–41]. The oxidation state of gold in the catalysts was investigated using XPS and the results of XPS for the supported Au/ZrO_2-nanocomposite (0.73 wt.% Au) catalyst before and after reaction are shown in Fig. 5.

The binding energy in Au 4*f* region for the as-prepared sample is shown in dash line in Fig. 5. The peak at 92.2 eV was assigned to $4f_{5/2}$ of Au^{3+} and the peak at 83.6 eV assigned to $4f_{7/2}$ of Au^0 are observed in the figure, suggesting that a fraction of gold in the Au/ZrO_2-nanocomposite (0.73 wt.% Au) exists in an oxidized Au^{3+} state prior to the catalytic reaction. Interestingly, most Au^{3+} became Au^0 and Au^+ (the peak at 89.2 eV is assigned to $4f_{5/2}$ of Au^+) during the reaction. It means that gold species were reduced by HCHO when the reactor was heated because the metallic gold is more stable at high temperature.

The changes of gold species during the catalytic reaction can also be observed in TEM results. In the TEM image of as-prepared Au/ZrO_2-nanocomposite catalyst (Fig. 6a) gold crystals cannot be observed, which are usually dark and have defined edges as shown in Fig. 6b. However, energy dispersive X-ray spectrum (EDS) from the selected area (in the rectangle) in Fig. 6a indicates the existence of gold element (Fig. 7). Therefore, in the as-prepared catalyst gold exist in a form of gold hydroxide or oxide rather than gold metal nanocrystals only. In the used catalyst (0.73 wt.% Au), gold crystals with the sizes between 3 and 10 nm are observed (Fig. 6b), which are not homogeneous compared with that reported in literature [35].

TEM observations and the EDS results are consistent with the XPS results that gold exists in an Au^{3+} state in the as-prepared catalyst and they were reduced to metallic crystals during the catalytic oxidation of HCHO. Nonetheless, gold in both states on ZrO_2-composite support are active for HCHO oxidation. The oxidation takes place at much lower temperatures on as-prepared and used Au/ZrO_2-nanocomposite catalysts than on ZrO_2-composite support. This is an interesting phenomenon in the point of view of the catalytic reaction mechanism. To understand the mechanism of the oxidation, the HCHO temperature programmed desorption on the as-prepared and the used catalysts were carried out.

3.4. HCHO temperature programmed desorption (TPD)

The HCHO TPD on Au/ZrO_2-nanocomposite (0.73Au) and the ZrO_2-nanocomposite support are depicted in Fig. 8.

The HCHO desorption peak at 325 K (peak 1) can be observed for both samples, and an additional peak at 380 K (peak 2) can be observed only for gold catalyst. The desorption peak at lower temperature is due to weak adsorption of HCHO on the support by Van der Waals force which cannot results in the oxidation reaction. While the desorption peak at higher temperature is from relatively stronger adsorption of HCHO on gold species by chemical

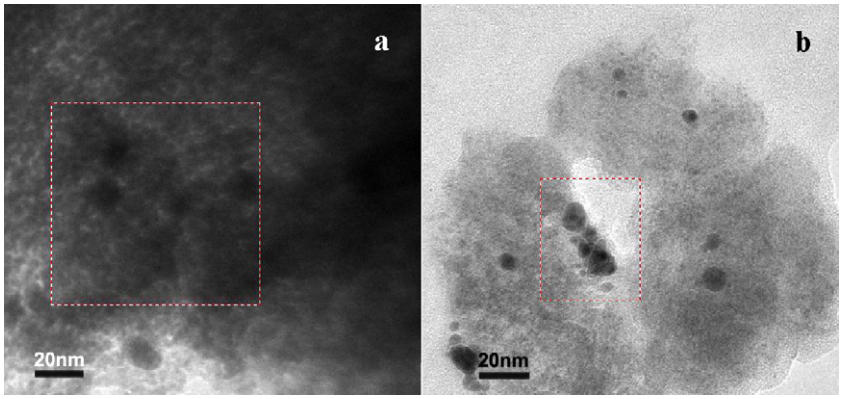

Fig. 6. TEM image of Au/ZrO_2-nanocomposite containing 0.73 wt.% Au: (a) As-prepared catalyst and (b) used catalyst.

adsorption which can promote the HCHO oxidation. Mao and Vannice reported that for the HCHO adsorption on the surface of Ag (Ag/α-SiO_2) by FTIR, a formate form was observed [42]. The HCHO adsorption on gold species is most likely analogous to that on silver, being chemically adsorbed formate.

3.5. TPSR (reaction of HCHO oxidation)

The results of TPSR study are shown in Fig. 9. In the case of trace a, HCHO was carried to the catalyst by purified air, followed by introducing high purity nitrogen. The HCHO oxidation took place in high purity nitrogen so that the reactant O_2 can only comes from the adsorbed oxygen. In the case of trace b, HCHO was introduced to catalyst by high purity helium, followed by introducing high purity nitrogen, so that no oxygen was introduced to the catalyst in this case. For the first case, broad CO_2 peaks at about 350 K and 450 K, respectively, can be observed on trace a, indicating that the HCHO oxidation proceeded considerably in that case. The two peaks could be attributed to the reactions between HCHO absorbed on different gold species, such as Au^{3+}, gold clusters or large gold crystals, and oxygen absorbed on the support [43]. No peaks can be observed in trace b because HCHO was carried by helium and no oxygen was introduced later. The oxidation could not take place without necessary oxidant.

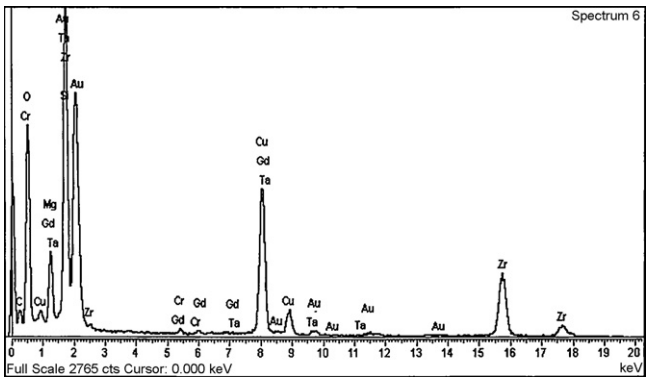

Fig. 7. EDS of the rectangle area in Fig. 5a.

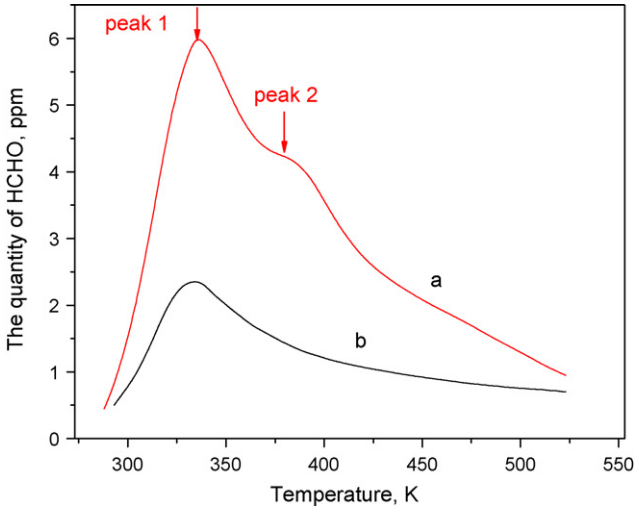

Fig. 8. TPD (temperature program desorption) graph: (a) (0.73Au) gold catalyst (containing both Au^{3+} and Au^0) and (b) the ZrO_2-composite support.

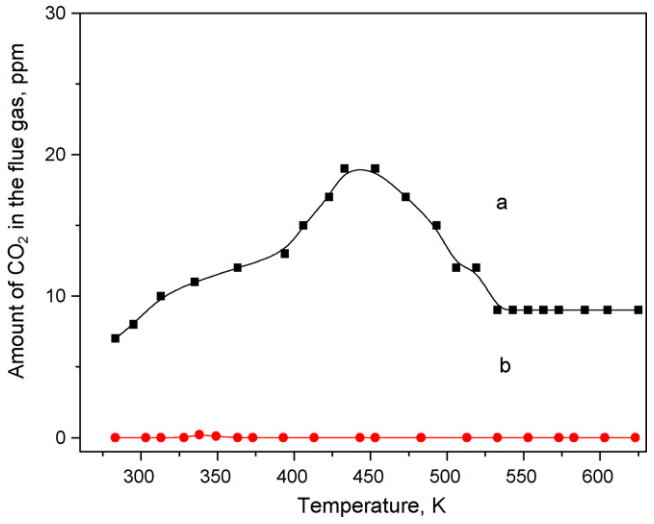

Fig. 9. TPSR profile of Au/ZrO_2-nanocomposite catalysts (0.73Au). Trace (a) was obtained when HCHO was oxidized in helium but adsorbed oxygen was available and trace (b) represents the situation when HCHO was oxidized in helium without adsorbed oxygen.

4. Discussion

4.1. The catalyst

There are several interesting new findings in this study. First, gold can be loaded onto the mesoporous composite and exists in a state of Au^{3+} (XPS result and TEM image). Gold was loaded in an environment with increased pH. In such environment ZrO_2-nanocomposite may restore the ion exchange ability, similar to

the pillared clays [34]. This may be beneficial for the existence of gold species in Au^{3+} state. Second, Au^{3+} species in the catalyst were reduced to metallic gold Au^0 during HCHO oxidation. Finally, both Au^{3+} and Au^0 are active species in the supported gold catalyst. The catalytic performance and adsorption behavior of the two species in catalysts are similar, according to the results of catalytic activity, TPSR and TPD experiments. In addition, the catalyst was used repeatedly in 2 months, no obvious deactivation was observed, indicating a good stability of the catalyst

4.2. The adsorption of reactants

The chemical adsorption of reactants on catalysts is usually the first and essential step of a catalytic reaction. The HCHO adsorption results indicate that gold species, in both Au^{3+} and Au^0 states, can adsorb HCHO molecules strongly (Fig. 8). But the adsorbed species are possibly in a formate form rather than HCHO molecules, similar to the situation of adsorption on silver particles [42], where COO group was discovered when HCHO was adsorbed on Ag/α-SiO_2 catalyst by FTIR

Moreover, TPSR results indicated the adsorbed oxygen is essential in the oxidation reaction. It has been reported that oxygen is adsorbed on the lattice vacancies of support [44]. In this work, the support is ZrO_2-nanocomposite in which ZrO_2 exists in small poorly crystallized nanoparticles (showing broad humps rather than sharp peaks in XRD pattern). There are lots of lattice vacancies in the support, which facilitate the adsorption of oxygen.

5. Conclusions

Mesoporous ZrO_2-nanocomposite is found to be a superior catalyst support and gold can be loaded on this support by a convenient deposition–precipitation method. As indicated by TEM image, in the as-prepared Au/ZrO_2-nanocomposite gold species are well dispersed over the support and exist in Au^{3+} oxidation state as shown by XPS. During the catalytic oxidation of HCHO on the catalyst Au/ZrO_2-nanocomposite, the gold in the high oxidation state (Au^{3+}) is reduced to metallic gold nanocrystals Au^0. Gold in both Au^{3+} and Au^0 states are active species for HCHO oxidation, and HCHO is strongly adsorbed on the gold species in both states to form adsorbed formate as proved by TPD and TPSR results. On the other hand oxygen adsorbed on the lattice vacancies of support is also important, which reacts with the formate adsorbed on the surface of gold to form the product CO_2. This study produced useful knowledge for the design of efficient supported gold catalysts for diverse applications.

Acknowledgements

Financial support for this work came from the National Science Foundation of China (20263001), from the Australian Research Council (ARC), the Endeavour Australia Cheung Kong Research Fellowship 2009, the starting foundation for young researchers of Inner Mongolia University (207037) and the research foundation from the Department of Education of Inner Mongolia Autonomous Region (NJZY07013).

References

[1] M. Haruta, N. Yamada, T. Kobayashi, J. Catal. 115 (1989) 301.
[2] N.A. Hodge, C.J. Kiely, R. Whyman, Catal. Today 72 (2002) 133.
[3] S.J. Lee, A. Gavriilidis, J. Catal. 206 (2002) 305.
[4] D.A. Bulushev, L. Kiwi-Minsker, I. Yuranov, J. Catal. 210 (2002) 149.
[5] S. Scire, S. Minico, C. Crisafulli, C. Satriano, A. Pistone, Appl. Catal. B 40 (2003) 43.
[6] M.A. Centeno, M. Paulis, M. Montes, Appl. Catal. A 234 (2002) 65.
[7] S. Scire, S. Minico, C. Crisafulli, J. Catal. Comm. 2 (2001) 229.
[8] M. Haruta, Catal. Today 36 (1997) 153.
[9] G.C. Bond, Catal. Today 72 (2002) 5.
[10] H.H. Kung, M.C. Kung, C.K. Costello, J. Catal. 216 (2003) 425.
[11] N. Lopez, T.V.W. Janssens, B.S. Clausen, Y. Xu, M. Mavrikakis, T. Bligaard, J.K. Norskov, J. Catal. 223 (2004) 232.
[12] F. Moreau, G.C. Bond, A.O. Taylor, J. Catal. 231 (2005) 105.
[13] D.B. Akolekar, S.K. Bhargava, G. Foran, M. Takahashi, J. Mol. Catal. A 238 (2005) 78.
[14] P.X. Huang, F. Wu, B.L. Zhu, X.P. Gao, H.Y. Zhu, T.Y. Yan, W.P. Huang, S.H. Wu, D.Y. Song, J. Phys. Chem. B 109 (2005) 19169.
[15] G.J. Hutchings, Catal. Today 100 (2005) 55.
[16] H.Y. Zhu, Z.P. Hao, J.C. Barry, Chem. Comm. (2002) 2858.
[17] H.Y. Zhu, J. Orthman, J.Y. Li, J.C. Zhao, G.J. Churchman, E.F. Vansant, Chem. Mater. 14 (2002) 5037.
[18] J.J. Spivey, Ind. Eng. Chem. Res. 26 (1987) 2165.
[19] International Agency for Research on Cancer, IARC Monographs on the Evaluation of the Carcinogenic Risk of Chemicals to Humans, Some Industrial Chemicals and Dyestuffs, Lyon, France, 29 (1982) 416.
[20] Agency for Toxic Substances and Disease Registry, Public Health Service, U.S. Department of Health and Human Services, Toxicological Profile for Formaldehyde, NTIS Accession No. PB99-166654 (1999) 451.
[21] J.A. Swenbenrg, W.D. Kerns, R.I. Mitchell, Cancer Res. 40 (1980) 3398.
[22] V.S. Engleman, Metal Fin. 98 (2000) 433.
[23] P. Papaefthimiou, T. Ioannides, X.E. Verykios, Appl. Catal. B 13 (1997) 175.
[24] E.M. Cordi, J.L. Falconer, J. Catal. 162 (1996) 104.
[25] N.E. Quaranta, J. Soria, V.C. Corberan, J.L.G. Fierro, J. Catal. 171 (1997) 1.
[26] J. Schwank, Gold. Bull. 16 (1983) 103.
[27] S. Minicò, S. Scirè, C. Crisafulli, S. Galvagno, Appl. Catal. B 34 (2001) 277.
[28] M. Haruta, A. Ueda, S. Tsubota, R.M. Torres Sanchez, Catal. Today 29 (1996) 443.
[29] C.Y. Li, Y.N. Shen, M.L. Jia, S.S. Sheng, M.O. Adebajo, H.Y. Zhu, Catal. Comm. 9 (2008) 355.
[30] Y.N. Shen, X.Z. Yang, Y.Z. Wang, Y.B. Zhang, H.Y. Zhu, L. Gao, M.L. Jia, Appl. Catal. B 79 (2008) 142.
[31] X. Yang, Y. Shen, L. Bao, H. Zhu, Z. Yuan, React. Kinet. Catal. Lett. 93 (2008) 19.
[32] H.Y. Zhu, J.C. Zhao, J.W. Liu, X.Z. Yang, Y.N. Shen, Chem. Mater. 18 (2006) 3993.
[33] M.L. Jia, Y.N. Shen, C.Y. Li, Z. Bao, S.S. Sheng, Catal. Lett. 99 (2005) 235.
[34] H.Y. Zhu, S.J. Yamanaka, Chem. Soc. Faraday Trans. 93 (1997) 477.
[35] V. Idakiev, T. Tabakova, A. Naydenov, Z.Y. Yuan, B.L. Su, Appl. Catal. B 63 (2006) 178.
[36] J.G. Carriazo, L.M. Martinez, J.A. Odriozola, S. Moreno, R. Molina, M.A. Centeno, Appl. Catal. B 72 (2007) 157.
[37] E.D. Park, J.S. Lee, J. Catal. 186 (1999) 1.
[38] R.D. Waters, J.J. Weimer, J.E. Smith, Catal. Lett. 30 (1994) 181.
[39] Y.M. Kang, B.Z. Wan, Catal. Today 26 (1995) 59.
[40] C.J. Jones, D. Taube, V.R. Ziatdinov, R.A. Periana, R.J. Nielsen, J. Oxgaard, W.A. Goddard, Angew. Chem. Int. Ed. 43 (2004) 4626.
[41] D. Briggs, M.P. Seah, Auger and X-ray Photoelectron Spectroscopy, Wiley, New York, 1990.
[42] C.F. Mao, M.A. Vannice, J. Catal. 154 (1995) 230.
[43] C.W. Chiang, A.Q. Wang, C.Y. Mou, Catal. Today 117 (2006) 220.
[44] M.M. Schubert, S. Hackenberg, A.C. van Veen, M. Muhler, V. Plzak, R.J. Behm, J. Catal. 197 (2001) 113.